PROCEEDINGS OF THE ROYAL SOCIETY A MATHEMATICAL, PHYSICAL & ENGINEERING SCIENCES

Structures in the microwave background radiation

Krzysztof A. Meissner, Pawel Nurowski and Blazej Ruszczycki

Proc. R. Soc. A 2013 **469**, 20130116, published 15 May 2013

PROCEEDINGS OF THE ROYAL SOCIETY A

rspa.royalsocietypublishing.org

Research

Cite this article: Meissner KA, Nurowski P, Ruszczycki B. 2013 Structures in the microwave background radiation. Proc R Soc A 469: 20130116.
http://dx.doi.org/10.1098/rspa.2013.0116

Received: 18 February 2013
Accepted: 15 April 2013

Subject Areas:
cosmology

Keywords:
microwave background radiation, origin and formation of the Universe, cosmology

Author for correspondence:
Błażej Ruszczycki
e-mail: b.ruszczycki@nencki.gov.pl

Structures in the microwave background radiation

Krzysztof A. Meissner[1], Paweł Nurowski[2] and Błażej Ruszczycki[3]

[1]Faculty of Physics, University of Warsaw, Hoża 69, 00-681 Warsaw, Poland
[2]Center for Theoretical Physics of the Polish Academy of Sciences, Al. Lotników 32/46, 02-688 Warsaw, Poland
[3]Nencki Institute of Experimental Biology, Polish Academy of Sciences, Pasteura 3, 02-093 Warsaw, Poland

We compare the actual Wilkinson microwave anisotropy probe maps with artificial, purely statistical maps of the same harmonic content to argue that there are, with confidence level 99.7 per cent, ring-type structures in the observed cosmic microwave background.

1. Introduction

Since its discovery, cosmic microwave background radiation (CMB) has been the subject of very intensive research. CMB anisotropy provides invaluable information not only about the Universe in the epoch of last scattering but also about earlier epochs. It follows from the lucky coincidence that before the last scattering the Universe was radiation dominated, and in the presence of radiation pressure it could not evolve and all the structures essentially remained frozen. Therefore, although the temperature at the last scattering was rather low (approx. 1 eV), searching for structures of different types in the CMB anisotropy can reveal facts about physics at energies far above those presently accessible in accelerators (approx. 10 TeV) reaching possibly even the Planck scale (approx. 10^{18} GeV).

In this paper, we compare the real CMB maps in three frequency sub-bands W1–W3 as measured by Wilkinson microwave anisotropy probe (WMAP) maps [1] with artificially produced purely Gaussian maps of the same harmonic spectrum, looking for possible ring-type structures in the temperature distribution (see Penrose [2] for a theoretical motivation). In this comparison, we used the HEALPix code [3] to visualize and handle the maps but we used our own code, described below, to

produce artificial maps. We find at least two statistically significant ring-type structures on the real maps (both happen to be on the southern Galactic Hemisphere) that have no analogues on the artificial maps. We compare several characteristics of the real maps and the artificial maps and it turns out that they significantly differ. We applied a quantitative test to measure the difference and it allowed us to conclude that with confidence level exceeding 99.7 per cent the ring-type structures we find on the real CMB maps are not the result of a statistical fluctuation.

2. Creation of artificial maps

Our algorithm for obtaining the maps with artificial CMB temperature distribution (with given power spectrum coefficients C_l) consists of the following:

1. We choose a maximal multipole number L (in the present paper, we use $L = 1000$).
2. For each multipole number l, $0 \leq l \leq L$, a positive integer N_l, which is the number of spherical harmonics contributing to the temperature for this given l (in the present paper, we used $N_l = 50 + 2l$).
3. For all integers k_l, $1 \leq k_l \leq N_l$, we assign a direction $(\theta_{k_l}, \phi_{k_l}) = (\arccos(2x_{k_l} - 1), 2\pi y_{k_l})$, where x_{k_l} and y_{k_l} are random numbers from the uniform distribution in the interval $[0, 1]$.
4. We take the coefficient C_l from the known real WMAP spectrum, and define a function $T_l = T_l(\theta, \phi)$ on the sphere by:
$$T_l(\theta, \phi) = \sqrt{\frac{C_l}{N_l}} \sum_{k_l=1}^{N_l} P_l(\cos(\omega(\theta, \phi, \theta_{k_l}, \phi_{k_l}))), \tag{2.1}$$
where $\omega(\theta, \phi, \theta_{k_l}, \phi_{k_l})$ is the spherical angle between a given point (θ, ϕ) on the sphere and the direction $(\theta_{k_l}, \phi_{k_l})$.
5. We repeat points (2)–(4) for each l, $1 \leq l \leq L$.

The final formula for the temperature on the artificial map is

$$T(\theta, \phi) = \sum_{l=0}^{L} T_l(\theta, \phi).$$

It depends on our choice of the integers L and the N_l's. There is no preferred direction on the sky, because, for each l, we choose randomly N_l directions $(\theta_{k_l}, \phi_{k_l})$ (therefore, this procedure has the advantage over averaging over m in the standard approaches). If we now perform the usual harmonic analysis of this map, then we get a set of C_l's that differ from the WMAP C_ls used in the procedure, but the difference can be made as small as we wish with the choice of sufficiently large N_l's (the deviation scales as $1/\sqrt{N_l}$). The artificial maps produced in this way are random Gaussian and, by the appropriate choice of N_l, can reproduce the prescribed spectrum of C_l with any required accuracy.

Because the spectrum of C_l obtained from the real maps is (especially for small l) not precisely known, we have produced artificial maps along the average, the upper and the lower C_l curve. For all of them, we obtained essentially the same result.

3. Looking for ring-type structures

In this section, we present a procedure applied to look for the ring-type structures. The idea consists of the following: we choose a function of the polar angle (and independent of the azimuthal angle) that vanishes from $\theta = 0$ to $\gamma_k - \epsilon$, is negative from $\gamma_k - \epsilon$ to γ_k, positive from γ_k to $\gamma_k + \epsilon$ and vanishes again for larger values of θ. The negative and positive values are chosen in such a way that the integral of this function over a sphere vanishes and the integral over only the positive part is the same for all γ_k's. Then, we integrate a product of this function with the temperature on the sky with the centre of the ring pointing in various directions and we gather

all the results of the integration. We carry out this procedure for different values of γ_k and ϵ, for all artificial maps and three bands of real maps and make the histograms for the values of the integrals. Then, from the artificial map distributions, we obtain a 'theoretical' cumulative distribution function for the values of the integrals for different ϵ (whereas different γ_ks are combined in the same histogram). We then apply the results of Meissner [4] to quantify the probability of obtaining large (in comparison with the artificial maps) values of the integrals that we observed on the three real maps.

We have excluded from all the maps the Milky Way belt (± 0.4 radians above and below the Galactic equator) to avoid introducing structures caused either by the Milky Way contribution or by the subtraction procedure usually applied to the CMB maps.

The procedure for looking for the ring-type structure for any given real or artificial map consisted of the following.

1. A grid of points with HEALPix ($k=6$) parametrization spreading over the entire sphere has been created.
2. A function $\Theta_{\epsilon,\gamma_k}(\gamma)$

$$\Theta_{\epsilon,\gamma_k} = \begin{cases} -(\cos(\gamma_k-\epsilon)-\cos\gamma_k)^{-1}, & \gamma_k-\epsilon<\gamma<\gamma_k \\ (\cos(\gamma_k)-\cos(\gamma_k+\epsilon))^{-1}, & \gamma_k<\gamma<\gamma_k+\epsilon \\ 0, & \text{otherwise,} \end{cases}$$

   is defined (this form is dictated by the area measure on the sphere and the condition that a constant temperature should give no contribution to the integral below.)
3. For N_d ($N_d \approx 7000$) directions (θ^i,ϕ^i) ($i=1,\ldots,N$) belonging to the grid, for all widths of rings ϵ ($\epsilon = 0.02$, 0.04 or 0.08 radians) and for all angular 'radii' $\gamma_k = 0.07 + 0.01k$ ($k=1,\ldots,23$) an integral

$$I_{(\epsilon,\gamma_k)}(\theta^i,\phi^i) = \int \mathrm{d}\Omega' \Theta_{\epsilon,\gamma_k}(\omega(\theta^i,\phi^i,\theta',\phi'))T(\theta',\phi')$$

   was calculated, $(\omega(\theta^i,\phi^i,\theta',\phi')$ is the spherical angle between (θ^i,ϕ^i) and $(\theta',\phi'))$. In this way, for a given ϵ we get a set of $N_d \cdot 23 \approx 160\,000$ values $I_{(\epsilon,\gamma_k)}(\theta^i,\phi^i)$.
4. For a given ϵ we take $N_d \cdot 23$ values of $I_{(\epsilon,\gamma_k)}(\theta^i,\phi^i)$ (separately for positive and negative values, about $N \sim 80\,000$ each), we make two histograms by grouping the values in n ($n=1500$) bins with centres x_i (i.e. the height of each bin is about 50 on average) and, for all artificial maps, we form the normalized cumulative distributions $F^{\pm}_m(x_i)$ ($+$ and $-$ stand for positive (negative) set, m stands for the map number and i stands for the bin number).
5. At each x_i, we average over all $F^{\pm}_m(x_i)$ to arrive at the average distribution $F^{\pm}(x_i)$.
6. We use the procedure for comparison of cumulative distribution functions introduced in Meissner [4]: for all artificial and three real maps W1–W3, we calculate

$$A = -\frac{a}{N}\sum_{i=1}^{n} d_i \ln(1-(F(x_i))^a), \tag{3.1}$$

   where a is a positive number (we used several numbers, all much larger than n) and d_i is the number of points in the ith bin (i.e. for how many points on a given map the value of the integral was close to x_i) therefore $\sum d_i = N$. Then, separately for positive and negative distributions, we check the hypothesis that a given map belongs to the distribution $F(x)$ using formula (16) given in Meissner [4]—the formula quoted there is suitable because it allows for quantitative comparison of distribution functions differing mostly at the tails (as is the case here).

The shape of the function $\Theta_{\epsilon,\gamma_k}(\theta^i,\phi^i)$ defines what we mean by the ring-type structure—the maximal integral is when the temperature is of the same shape. Because we gather in the same

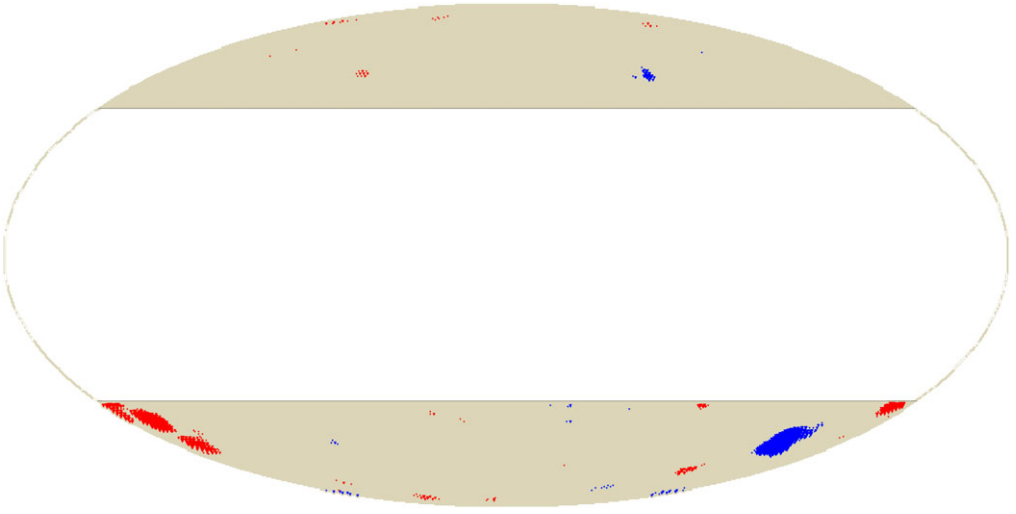

Figure 1. Position of centres of circular structures on the real maps W1–W3.

histogram all values of γ_k, the same direction can give several large values of the integral, so these values can be correlated. The division into smaller number of bins n ($n \ll N \cdot 23$) is intended to partially compensate for these correlations.

4. Results

It is commonly taken for granted (with the notable exception of Gurzadyan & Penrose [5]) that the temperature distribution in the CMB is purely statistical being produced by the quantum fluctuations usually assumed to have taken place during inflation (as evolution of quantum fields in De Sitter space suggests). Therefore, it was very unexpected for us to find significant differences (with confidence level 99.7%) between the WMAP results and artificial maps (with the same power spectrum as the real WMAP maps) that we have created. We believe that the procedure of creating artificial maps described earlier, being different from the one usually used, is interesting on its own. It gives random Gaussian maps with the prescribed harmonic content of any desired accuracy.

We have produced many artificial maps (generation of an artificial map with our procedure is fast), but the procedure for looking for ring-type structure required the number of integrals for any given map to be very large ($N \cdot 23 \approx 160\,000$), and the CPU time needed was the main reason to limit ourselves in the present paper to 100 artificial maps only.

The differences between real and artificial maps were both qualitative and quantitative. First of all, for $\epsilon = 0.08$ on frequency sub-band maps W1–W3, we find two directions around which there is a significant concentration of circular structures distinguished by the large values of $I_{(\epsilon,\gamma_0)}(\theta,\phi)$. The Galactic coordinates of these two directions are approximately $(\tilde{\theta}_1, \tilde{\phi}_1) = (2.6, 3.7)$ (which correlates with the so-called cold spot [6–8]) and $(\tilde{\theta}_2, \tilde{\phi}_2) = (2.6, 2.9)$ (this is new and has opposite values of the integral—the highest values from this direction are shown in figure 2). We interpret these two directions as two centres of circular rings in the temperature distribution. The reason for this interpretation is as follows: in the close vicinity (about 8×10^{-3} sr) of the first of these directions, there are about 80 centres of circular structures (and there are none immediately outside). A similar situation occurs around the second direction—there we find about 40 centres in about the same solid angle as in the first case.

The quantitative comparison between the real W1–W3 maps with the artificial maps regarding the existence of structures with $\epsilon = 0.08$ yields the following:

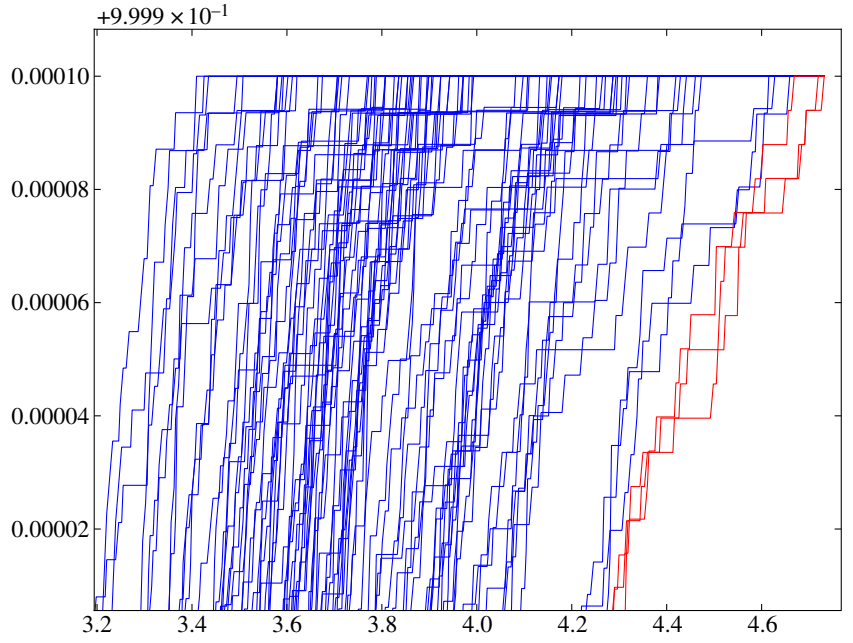

Figure 2. The tail of the distributions of the integrals of the 100 artificial (blue) and three real (red) maps. Abscissa: normalized values of $I_{(\epsilon,\gamma_k)}(\theta^i, \phi^i)$. Ordinate: cumulative distribution function.

For the procedure described earlier, we get for the real maps W1–W3 with $n = 1500$, $a = 3\,000\,000$ the values $A = 107.9$, 133.5, 84.8, respectively, whereas only six of 100 artificial maps have $A > 1$ (the largest value among these six maps is $A \approx 52$, the other five have much smaller A). To take into account possible correlations (we gather in the same histogram the values of integrals for many different γ_k's), from the distribution of A in the artificial maps, we fitted the parameter α in the formula (16) of Meissner [4] describing the probability of A bigger than σ for large α:

$$P(A > \sigma) \sim 1 - \left(1 - \exp\left(-\frac{\sigma}{\alpha}\right)\right)^{1/\alpha}. \tag{4.1}$$

We expect that because of the correlations the fitted α should be smaller than $a/n = 2000$ and bigger than $a/N \sim 37$. In the case at hand, the fitted $\alpha \sim 83$. Plugging the value from the real map W2, i.e. $\sigma = 133.5$ the probability of a statistical fluctuation is $\approx 0.3\%$ (the value for two other sub-bands is very similar). It means that with 99.7 per cent confidence level we can reject the hypothesis that the values of the integrals on the real maps are purely statistical and state that the ring-type structures on the background radiation maps are not statistical fluctuations (it is important to note that we obtained the same result also for smaller values of α). In favour of this statement, we can also observe that for the value of $I_{(\epsilon,\gamma_0)}(\theta, \phi)$ greater than 3 on the map of frequency band W2 only 81 points are in the northern Galactic Hemisphere and 1430 in the Southern one—the difference is similar for two other spectral types, but there are no such differences for the artificial maps.

It is interesting to note that for $\epsilon = 0.02$ and $\epsilon = 0.04$ the differences between the real and artificial maps are much smaller than for $\epsilon = 0.08$. In Gurzadyan & Penrose [5], the characteristic value of rings is around 0.5° and in our case 5°—it is not clear that we observe the same effect (the circles of variance there and the 'derivatives of the delta function' in our case) but statistical insignificance of small ϵ in our case may be due to very large coefficients of the power spectrum corresponding to these small angles what may hide the presence of circles for such small angles in the averaging procedure caused by grouping the values in histograms. We hope to apply our procedure to the Planck data to clear this issue.

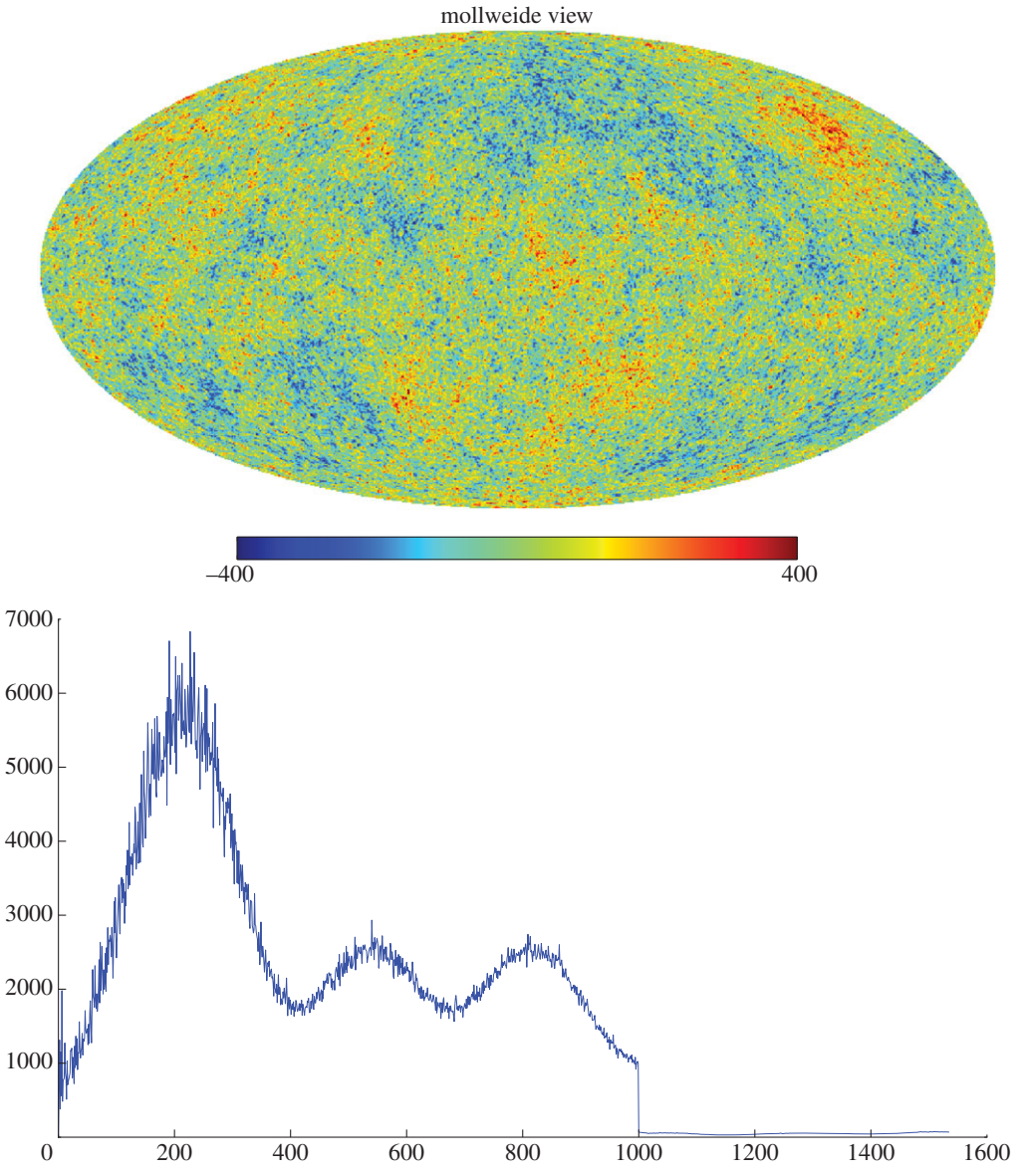

Figure 3. One of our artificial maps and its power spectrum.

For comparison, we have also imposed a condition that around the same direction (θ, ϕ), and we have both large positive and large negative integrals. It turned out that none of the real maps shows any statistically significant presence of such structures—it points to the presence of one sharp circular edge in the temperature distribution and not two or more (which may be there but milder).

In figure 1, we have plotted the directions of the suspected ring-type structures on the real WMAP maps in three frequency bands W1–W3 (with the galactic disc excluded, as described in the text). In figure 2, we have plotted the upper part of the histogram of the cumulative distribution functions for all artificial maps and three real maps W1–W3 (for positive value of the integral). In figure 3, we have given one of the artificial maps created by the algorithm described earlier and its calculated power spectrum.

We gratefully acknowledge helpful discussions with Paweł Bielewicz, Marek Demiański, Krzysztof Górski, Roger Penrose and K. Paul Tod. Special thanks are due to C. Denson Hill and E. Ted Newman for many suggestions on preliminary versions of the article. P.N. was partially supported by grant (no. N202 104838) and B.R. by POIG-008 grant.

References

1. Hinshaw G *et al*. 2007 Three-year Wilkinson microwave anisotropy probe (WMAP) observations: temperature analysis. *Astrophys. J. Suppl.* **170**, 288. (doi:10.1086/513698)
2. Penrose R. 2010 *Cycles of time: an extraordinary new view of the universe*. London, UK: Bodley Head.
3. Górski KM, Hivon E, Banday AJ, Wandelt BD, Hansen FK, Reinecke M, Bartelman M. 2005 HEALPix: a framework for high-resolution discretization and fast analysis of data distributed on the sphere. *Astrophys. J.* **622**, 759–771. (doi:10.1086/427976)
4. Meissner KA. 2012 A tail sensitive test for cumulative distribution functions. (http://arxiv.org/abs/1206.4000)
5. Gurzadyan VG, Penrose R. 2013 On CCC-predicted concentric low-variance circles in CMB sky. *Eur. Phys. J. Plus* **128**, 22–38. (doi:10.1140/epjp/i2013-13022-4)
6. Cruz M, Martinez-Gonzalez E, Vielva P, Cayon L. 2005 Detection of a non-Gaussian spot in WMAP. *Mont. Not. R. Astron. Soc.* **356**, 29–40. (doi:10.1111/j.1365-2966.2004.08419.x)
7. Cruz M, Cayon L, Martinez-Gonzalez E, Vielva P, Jin J. 2007 The non-Gaussian cold spot in the 3-year WMAP data. *Astrophys. J.* **655**, 11–20. (doi:10.1086/509703)
8. Zhang R, Huterer D. 2010 Disks in the sky: a reassessment of the WMAP 'cold spot'. *Astropart. Phys.* **33**, 69–74. (doi:10.1016/j.astropartphys.2009.11.005)